Far infrared and photoacoustic characterization of iodine doped PbTe

P. M. NIKOLIĆ*, K. M. PARASKEVOPOULOS[a], O. S. ALEKSIĆ[b], S. S. VUJATOVIĆ, D. VASILJEVIĆ-RADOVIĆ[c], T. T. ZORBA[a], V. BLAGOJEVIĆ[d], N. NIKOLIC[b], M. RADOVANOVIĆ[e], M. V. NIKOLIĆ[b]
Institute of Technical Science of SASA, Knez Mihailova 35, Belgrade, Serbia
[a]*Physics Department, Solid State Section, Aristotle University, Thessaloniki, Greece*
[b]*Institute for Multidiciplinary Research, University of Belgrade, Kneza Višeslava 1, Belgrade, Serbia*
[c]*ICTM-Centre of Microelectronic Technologies and Single Crystals, University of Belgrade, Njegoševa 12, Belgrade, Serbia*
[d]*Faculty of Electrical Engineering, University of Belgrade, Belgrade, Serbia*
[e]*Faculty of Technical Sciences,University of Novi Sad, Novi Sad, Serbia*

Single crystal samples of PbTe doped with PbI_2 were made using the Bridgman technique. Far infrared reflectivity diagrams of PbTe doped with 0.4 at% and 0.6 at% Iodine were measured and numerically analyzed. A plasma resonance at about 650 cm^{-1} with the reflectivity minima very close to zero was observed for both samples. Thermal diffusivity was determined for the same samples using the photoacoustic method with a transmission detection configuration and the values of the minority free carrier (holes) mobility were calculated.

(Received December 29, 2011; accepted April 11, 2012)

Keywords: Doped Semiconductors, Far Infrared Reflectivity, Photoacoustic Characterization.

1. Introduction

Recent publications have focused on revaluation of $PbTe_{1-x}I_x$ as a high performance thermoelectric material [1]. A large figure of merit (ZT) of 1.4 in the temperature range between 700 K and 850 K was confirmed, which is much larger than the value usually referenced for this material. One should say also that a higher value of the thermoelectric figure of merit, above 2, was recently reported for PbTe doped with both chromium and iodine [2].

The solubility of Iodine in lead telluride is rather high. Halogen solubility in $PbTe_{1-x}Hal_x$ increases similarly to the atomic weight of Cl, Br and I e.g. $X_{Cl}\approx0.03$, $X_{Br}\approx0.07$ and $X_I\approx0.09$ [3].

Doping PbTe with PbI_2, Al or Zr in order to optimize the carrier concentration of functional gradient materials was also investigated [4]. Far infrared properties of PbTe doped with Hg were investigated in [5].

In literature, as far as we know, there is no published infrared optical reflectivity data on PbTe doped with Iodine. So, in this work we have studied far and mid infrared optical reflectivity properties of PbTe doped with PbI_2. We also investigated thermal and electronic transport properties of the same PbTe + I samples using a photoacoustic (PA) method with the transmission detection configuration [6].

2. Experimental

Single crystal samples of $PbTe_{1-x}I_x$ were prepared from elementary tellurium of 99.999% purity, lead metal of 99.999% and PbI_2 of 99.998% purity. Since La Londe et al [1] showed that the Seebeck coefficient fot $PbTe_{1-x}I_x$ has the highest values for x between 0.01 and 0.0055 we made a sample starting with x = 0.01 using the standard Bridgman method [7]. The produced ingot was a single crystal with a sharp beginning of about 2 mm and useful ingot with a diameter of about 8 mm where the composition was about 0.6 at.% I that gradually decreased approaching the upper end to 0.4 at.% I. Samples were cleaved or cut from the ingot and then highly polished before they were used for structural, optical and photoacoustic measurements. X-ray diffraction of samples was used to prove that each sample was single crystal. EDS analysis (INCA Penta EDS system attached to a TESCAN VEGA TS 5130MM Electron Microscope) was used to determine the content of Pb, Te and I in each sample. It was proved that the concentration of Iodine slightly decreased from the top to the end of the ingot. Microstructural characterization was done by AFM (Thermo Microscopes, Autoprobe CP Research). All measurements were performed in the non-contact mode using a rectangular silicon cantilever (resonant frequency in the range 250-300 kHz, spring constant in the range 30-80 N/m). Far infrared reflectivity spectra of the PbTe samples doped with 0.6 at% - 0.4 at% of I were measured at room temperature using a Bruker IFS -113 V spectrometer. Photoacoustic (PA) amplitude and phase

spectra of the same samples were measured using a photoacoustic cell protected against the surrounding influence [8] and the experimental setup was described elsewhere [9].

3. Results and discussion

AFM images of the analyzed PbTe samples doped with Iodine are given in Fig. 1. One can see that the surface has relatively homogenous grains.

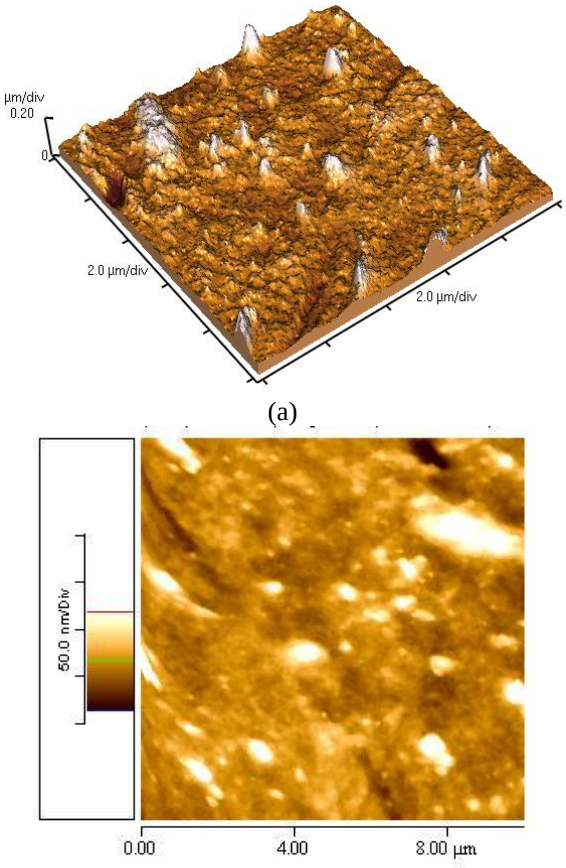

Fig. 1. AFM image of a PbTe sample doped with 0.4 at% I (a) 3D surface view; (b) 2D planar view.

Room temperature FIR reflectivity diagrams for two PbTe+I samples, one from the beginning and the other near the end of the ingot are given in Fig. 2a and Fig. 2b. For these samples a reflectivity minimum was observed at about 640 cm^{-1} and 650 cm^{-1}, respectively. Reflectivity minima (R_{min}) for both cases were approaching zero e.g. they were at about 0.01 and 0.02 respectively. The frequency marked by an arrow in Fig. 2a and Fig. 2b represents the position of the coupled Plasmon – longitudinal phonon (LO) modes. These experimental diagrams were numerically analyzed using the four parameter model introduced by Gervais and Piriou [10] and the optical parameters (plasma frequency - ω_p and its damping factor - γ) were determined. Their values for the mentioned two samples are given in Table 1. The values of their error bars were less than 1 cm^{-1}. The optical mobility (μ_{opt}) of the free carriers was calculated using the method of Moss et al. [11] and is also given in Table 1.

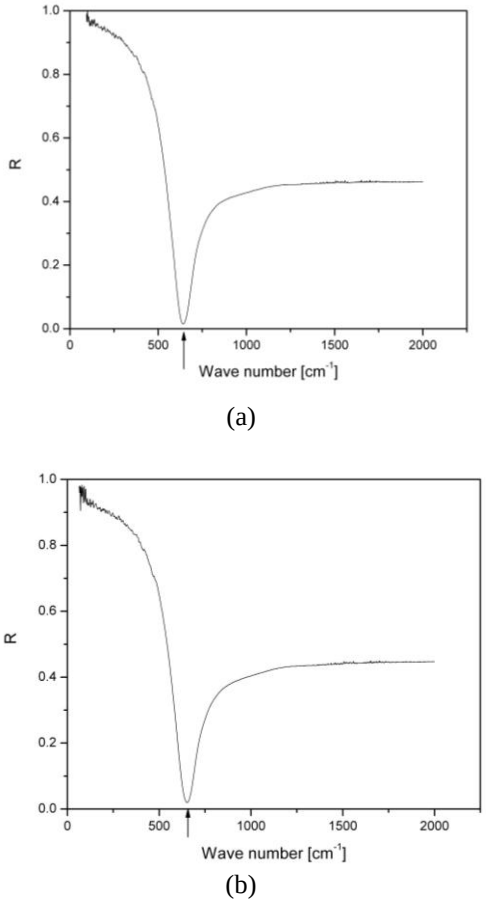

Fig. 2. Room temperature IR reflectivity diagrams for PbTe doped with 0.6 at.% I (a) and 0.4 at.% I (b).

Table 1. Optical parameters determined for PbTe+I samples (R_{min} – reflectivity minima; ω_p – plasma frequency; γ - damping factor for plasma frequency; μ_{opt} – optical mobility of free carriers).

PbTe +I	at% I	R_{min}	ω_p [cm^{-1}]	γ [cm^{-1}]	μ_{opt} [cm^2/Vs]
Pb5 beginning	0.6	0.01	637	72.1	600
Pb6 end	0.4	0.02	638	57	633

The values of free carrier mobility were also calculated by fitting photoacoustic measurements. The amplitude and phase spectra of these samples were measured using a specially constructed PA cell which had an optimized acoustic protection from the surrounding influence [12]. The optical source was a red laser (80 mW), which was modulated by a mechanical chopper. The

sample was irradiated by a spot 3 mm in diameter and it was mounted directly on the front of the electrets microphone. Both amplitude and phase spectra of the PA signals for both samples were measured for two different plate thicknesses. The initial thickness of sample 1 was 1.265 mm and then it was made thinner to 0.93 mm. The sample 2 was measured when it was 1.14 mm thick and after it was made thinner to 0.835 mm, and measured again. The different thicknesses were obtained by polishing one side of the thick plate with diamond paste and the other side was at first only flattened with silicon carbide with 1 μm grade and then made thinner. That surface was always illuminated with the modulated laser beam, while the side which was polished with diamond paste was always put on the front of the electrets' microphone. The measured amplitude and phase PA signals, versus the modulation frequency, for both samples are given in Fig. 3a and Fig. 3b, respectively. These measurements for two samples thicknesses were necessary for normalization of the PA amplitude and phase spectra as the sensitivity of the electrets' microphone decreases in the frequency range below 100 Hz, so we used the signal ratio for two different thicknesses of each measured sample. Beginning with the Rosencwaig-Gersho thermal piston model [13] the PA signal $S(-l, \omega)$ can be given with the following equation:

$$S(-l,\omega) = \gamma \frac{P_o \Phi(-l,\omega)}{T_o k_l l_b} \quad (1)$$

where γ is the adiabatic constant; P_o and T_o are the ambient pressure and temperature, respectively; $k_l=(1+j)/\mu_b$, where μ_b is the thermal diffusion length of the backing gas and l_b is the distance between the sample and the microphone. Finally $\Phi(-l, \omega)$ is the periodic temperature variation of the rear sample surface. The PA signal for two measurements and two different sample thicknesses can be normalized taking the signal ratio using the equation:

$$\frac{S_1(\omega)}{S_2(\omega)} = \left[\frac{\Phi(-l_1)}{\Phi(-l_2)}\right] e^{[j(\varphi_1(-l_1)-\varphi_2(-l_2)]} = A_m e^{j\Delta\varphi} \quad (2)$$

where $\Phi(-l)$ is the temperature distribution on the surface of the sample put in contact with the electrets microphone; A_m is the amplitude ratio and $\Delta\varphi$ is the phase difference of the measured PA signals for two different sample thicknesses of the same sample.

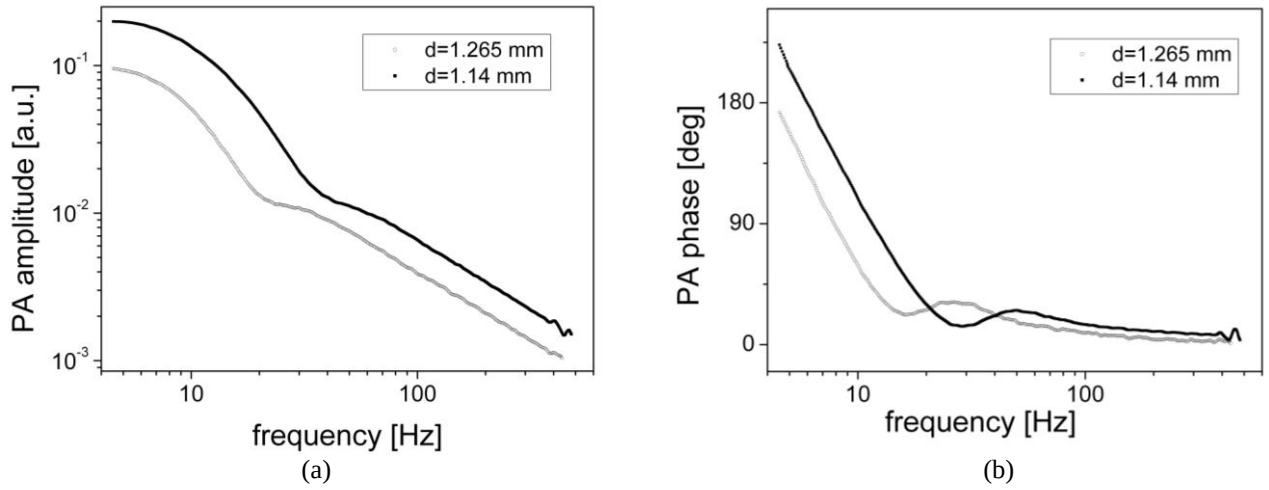

Fig. 3. PA amplitude (a) and phase spectra (b) for PbTe doped with 0.6 at.% I for two different sample thicknesses.

The amplitude ratio and phase difference of fitted diagrams for sample 2 and its two different thicknesses are given in Fig. 4a and Fig. 4b respectively. Values of the fitted parameters obtained during the fitting procedure for both sample 1 and sample 2 and their two normalized PA spectra are given in Table 2. The values of the following parameters were calculated: thermal diffusion coefficient (D_T), excess carrier life time (τ), the hole diffusion coefficient (D) and optical absorption coefficient (α) the calculated mobility of hole carriers (μ_h).

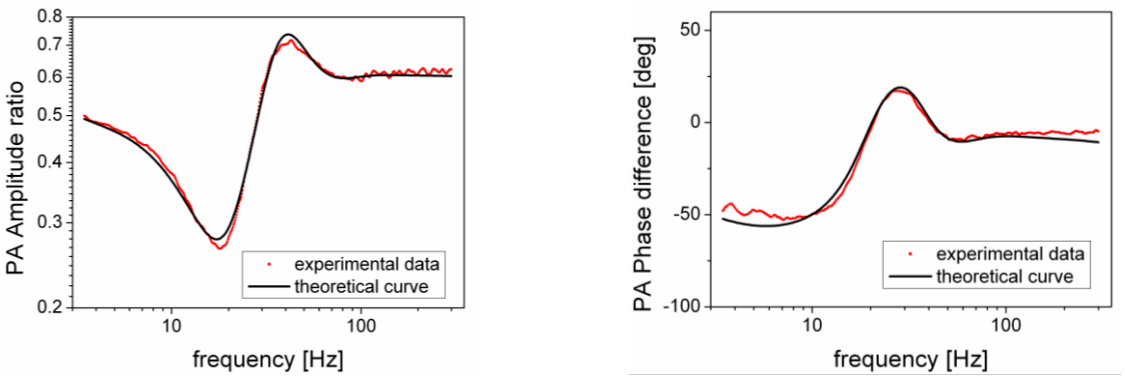

(a) (b)

Fig. 4. Experimental (points) and theoretically calculated (full line) PA amplitude (a) and phase difference (b) spectra of PbTe doped with 0.4 at.% I.

Table 2. Thermal parameters determined for PbTe+I samples.

Sample	I [at%]	D_T [m^2/s]	τ [μs]	D[m^2/s]	α [m^{-1}]	μ_h[cm^2/Vs]
Sample 1 1.26mm/0.93 mm	0.6	0.204×10^{-5}	0.041	0.266×10^{-2}	8647	1030
Sample 2 1.14mm/0.835 mm	0.4	0.19×10^{-5}	0.106	0.423×10^{-2}	30604	1640

The calculated values of the hole mobility are higher than for pure PbTe, and they are in agreement with the diagrams of room temperature carrier concentration dependence of Hall mobility for $PbTe_{1-x}I_x$ given by La Londe et al. [1]. They determined maximum hole mobility of about 2000 cm^2/Vs responding to carrier concentrations of free holes of about 10^{19} cm^{-3}. Since the thermal diffusivity coefficient (D_T) decreases when the atomic percentage of Iodine in PbTe decreases from 0.6 at% to 0.4 at% we can conclude that it is also in agreement with the change of the figure of merit (ZT) given in [1] where the best content of I is about 0.12 at%. The above conclusion is obvious if we mention that $D_T=K/dC_p$, where K is the thermal conductivity, C_p is the specific heat and d is density. But also having in mind that

$$ZT = \frac{S^2 T}{\rho(K_E + K_L)} \tag{3}$$

where S, ρ,K_E and K_h are the Seebeck coefficient, resistivity and electric and lattice components of thermal conductivity, respectively.

It is obvious that sample 2, doped with 0.4 at% I is slightly better than sample 1 doped with 0.6% having the hole mobility 1640 cm^2/Vs. The same sample also has a smaller thermal diffusivity coefficient (D_T) and thus a lower thermal conductivity K. The final result is that, for the sample of PbTe doped with 0.4 at% I, the figure of merit (ZT) is higher, that is in agreement with the results of La Londe [1]. A similar conclusion could be made using reference [14].

The effect of Iodine content (percentage) in PbTe is obviously very important because even the lattice parameter of $PbTe_{1-x}I_x$ has a non-monotonic function having a sharp minimum for a specific value of iodine content [15]. It is interesting that the thermoelectric properties of a double doped PbTe with Cd and Iodine was recently studied by Kyunghan et al [16] investigating possible increase of the Seebeck coefficient and they found that the optimal PbI_2 doping of the PbTe+1 at% CdTe for the best ZT was 0.055 mol%.

Iodine as a dopant in PbTe is mainly considered from the aspect of improving thermoelectric properties of PbTe. Furthermore, PbTe-Ge [17] and PbTe-Si [18] eutectic composites can be doped with PbI_2 with a precisely controlled carrier concentration. In this work we have shown that using optical reflection measurements in the plasma frequency resonance range one can get information on the concentration and mobility of free carriers. For higher free carrier concentrations the plasma minimum occurs at higher wave numbers and vice versa. The plasma frequency becomes narrower when the free charge carrier relaxation time decreases. The high frequency dielectric permeability can also be determined from the short wave part of the reflection spectrum. Similar properties can be obtained using photoacoustic measurements of the same samples.

4. Conclusion

In this work, as far as we know, far infrared optical reflectivity and photoacoustic properties of single crystal PbTe samples doped with PbI_2 between 0.4 at% I and 0.6 at% I were measured for the first time. We obtained the results which confirm literature data that a small percentage of Iodine, much less than 1 at% can

significantly improve thermoelectric and electrical properties of this doped semiconductor. From photoacosutic spectra we calculated the thermal diffusivity and hole diffusion coefficient and finally free hole mobility values. For PbTe doped with 0.4 at% I the free hole mobility was 1640 cm^2/Vs. Further decrease of the iodine content until an optimal concentration would result in further improved thermoelectric and electrical properties and possible application as a high performance thermoelectric material.

Acknowledgements

This work was performed within projects III45007 and III45014 financed by the Ministry for Science and Education of the Republic of Serbia.

References

[1] A. D. La Londe, Y. Z. Pei, G. Jeffrey Snyder Energy Environ. Sci., **4**, 2090 (2011).
[2] B. Paul, P. K. Rawat, P. Banerji, Appl. Phys. Lett. **98**, 262101 (2011).
[3] M. K. Sharov, O. B. Yatsenko, Y. A. Ugai, Inorganic Materials **42**, 723 (2006).
[4] Z. P. Wen, H. Y. Liang, W. Xin, C. L. Xue, I. Yoshio, Chinese Phys. Lett. **27**, 058102 (2010).
[5] P. M. Nikolić, S. S. Vujatović. K. M. Paraskevopoulos, E. Pavlidou, T. T. Zorba, T. B. Ivetić, O. Cvetković, O. S. Aleksić, V. D. Blagojević, M. V. Nikolić, Optoelectron. Adv. Mater. - Rapid Commun. **4**, 151 (2010).
[6] P. M. Nikolić, D. M. Todorović, A. I. Bojičić, K. T. Radulović, D. Urošević, J. Elazar, V. Blagojević, P. Mihajlović, M. Miletić, J. Phys. Condens. Matter **8**, 5673 (1996).
[7] B. A. Akimov, A. B. Nikorich, L. I. Ryabova, N. A. Shirokova, Fiz. Tekh. Poluprovodn., **23**, 1019 (1989).
[8] D. M. Todorović, P. M. Nikolić, Opt. Eng., **36**, 432 (1997).
[9] P. M. Nikolić, S. S. Vujatović, D. M. Todorović, M. B. Miletić, A. Golubović, A. I. Bojičić, F. Kermendi, S. Djuric, K. T. Radulović, J. Elazar, Jap. J. Appl. Phys., **36**, 1006 (1997).
[10] F. Gervais, B. Piriou, Phys. Rev. B, **10**, 1842 (1974).
[11] T. G. Moss, T. D. Hawkins, G. J. Burrell, J. Phys. C, **1**, 1435 (1968).
[12] P. M. Nikolić, D. M. Todorović, Proc. 20th Conf. Microelectronics MIEL 95, Niš, Serbia, **1**, 107 (1995).
[13] A. Rosencwaig, A. Gersho, J. Appl. Phys., **46**, 64 (1976).
[14] Z. H. Dughaish, Physica B, **322**, 205 (2002).
[15] Ya. A. Ugai, M. K. Sharov, O. B. Yatshenko, Inorganic Materials, **40**, 806 (2004).
[16] A. Kyunghan, M. K. Han, J. He , J. Androulakis, S. Ballikaya, C. Uher, V. P. David, M. G. Kanatzidis, J. Am. Chem. Soc., **132**, 5227 (2010).
[17] J. R. Sootsman, J. He, V. P. Dravid, C. –P. Li, C. Uher, M. G. Kanatzidis, J. Appl. Phys., **105**, 083718 (2009).
[18] J. R. Sootsman, J. He, V. P. Dravid, S. Ballikaya, D. Vermeulen, C. Uher, M. G. Kanatzidis, Chem. Mater., **22**, 869 (2010).

*Corresponding author: Pantelija.Nikolic@sanu.ac.rs